Research Article

Journal of Molecular Recognition

Received: 20 August 2012, Revised: 01 October 2012, Accepted: 12 November 2012, Published online in Wiley Online Library: 2012

(wileyonlinelibrary.com) DOI: 10.1002/jmr.2256

Allostery mediates ligand binding to Grb2 adaptor in a mutually exclusive manner

Caleb B. McDonald, Jimmy El Hokayem, Nawal Zafar, Jordan E. Balke, Vikas Bhat, David C. Mikles, Brian J. Deegan, Kenneth L. Seldeen and Amjad Farooq*

Allostery plays a key role in dictating the stoichiometry and thermodynamics of multi-protein complexes driving a plethora of cellular processes central to health and disease. Herein, using various biophysical tools, we demonstrate that although Sos1 nucleotide exchange factor and Gab1 docking protein recognize two non-overlapping sites within the Grb2 adaptor, allostery promotes the formation of two distinct pools of Grb2–Sos1 and Grb2–Gab1 binary signaling complexes in concert in lieu of a composite Sos1–Grb2–Gab1 ternary complex. Of particular interest is the observation that the binding of Sos1 to the nSH3 domain within Grb2 sterically blocks the binding of Gab1 to the cSH3 domain and vice versa in a mutually exclusive manner. Importantly, the formation of both the Grb2–Sos1 and Grb2–Gab1 binary complexes is governed by a stoichiometry of 2:1, whereby the respective SH3 domains within Grb2 homodimer bind to Sos1 and Gab1 via multivalent interactions. Collectively, our study sheds new light on the role of allostery in mediating cellular signaling machinery. Copyright © 2013 John Wiley & Sons, Ltd.

Keywords: Multivalent binding; intrinsic disorder; stoichiometry; steric hindrance; allosteric control

INTRODUCTION

Grb2 adaptor relays external signals from receptor tyrosine kinases (RTKs) at the cell surface to downstream effectors and regulators such as Ras and Akt within the cytosol (Gale *et al*., 1993; Li *et al*., 1993; Chardin *et al*., 1995; Nimnual and Bar-Sagi, 2002). Composed of the ubiquitous nSH3–SH2–cSH3 signaling module (Figure 1a), where the nSH3 and cSH3 are respectively the N-terminal and the C-terminal SH3 domains flanking the central SH2 domain, Grb2 recognizes activated RTKs by virtue of its SH2 domain's ability to bind to tyrosine-phosphorylated (pY) sequences in the context of pYXN motif located within the cytoplasmic tails of a diverse array of receptors, including EGF, FGF, and PDGF receptors (Lowenstein *et al*., 1992; Rozakis-Adcock *et al*., 1992; Rozakis-Adcock *et al*., 1993). Upon binding to RTKs, the SH3 domains of Grb2 present an opportunity for a wide spectrum of proline-rich (PR) proteins to be recruited to the inner membrane surface, the site of initiation of a plethora of signaling cascades (Chardin *et al*., 1993; Li *et al*., 1993; Seedorf *et al*., 1994; Odai *et al*., 1995; Park *et al*., 1998; Vidal *et al*., 1998; Schaeper *et al*., 2000; Lewitzky *et al*., 2001; Moeller *et al*., 2003). Among them, the Sos1 guanine nucleotide exchange factor and the Gab1 docking protein are by far the best-characterized downstream partners of Grb2 (Chardin *et al*., 1993; Egan *et al*., 1993; Adams *et al*., 1995; Schaeper *et al*., 2000; Lewitzky *et al*., 2001). Upon recruitment to the inner membrane surface, Sos1 facilitates the GDP–GTP exchange within the membrane-bound Ras GTPase and thereby switches on a key signaling circuit that involves the activation of MAP kinase cascade central to cellular growth and proliferation (Robinson and Cobb, 1997; Reuther and Der, 2000). In contrast, the recruitment of Gab1 to the inner membrane surface provides docking platforms for the Shp2 tyrosine phosphatase and the PI3K kinase, which respectively account for further amplification of Ras activity, as sustained activation of Ras requires both the Sos1-dependent and Gab1-dependent pathways (Yart *et al*., 2001; Cunnick *et al*., 2002; Araki *et al*., 2003; Gu and Neel, 2003; Gotoh, 2008; Eulenfeld and Schaper, 2009), and the activation of Akt serine–threonine kinase, which plays a pivotal role in cell growth and survival (Kim and Chung, 2002).

How exactly does Grb2 recruit Sos1 and Gab1 to the inner membrane surface? Although seminal work implicated the role of both SH3 domains of Grb2 in the recruitment of Sos1 to the inner membrane surface (Chardin *et al*., 1993; Egan *et al*., 1993; Li *et al*., 1993), we have previously shown that Grb2 primarily recognizes Sos1 through its nSH3 domain (McDonald *et al*., 2010). In contrast, the recruitment of Gab1 is driven through the binding of the cSH3 domain of Grb2 (Lock *et al*., 2000; Lewitzky *et al*., 2001). More importantly, our recent work has

* *Correspondence to: Amjad Farooq, Department of Biochemistry and Molecular Biology, Leonard Miller School of Medicine, University of Miami, Miami, FL 33136, USA. E-mail: amjad@farooqlab.net*

C. B. McDonald, J. El Hokayem, N. Zafar, J. E. Balke, V. Bhat, D. C. Mikles, B. J. Deegan, A. Farooq
Department of Biochemistry and Molecular Biology, Leonard Miller School of Medicine, University of Miami, Miami, FL, 33136, USA

Abbreviations: *ALS, analytical light scattering; CD, circular dichroism; DLS, dynamic light scattering; EGF, epidermal growth factor; FGF, fibroblast growth factor; Gab1, Grb2-associated binder 1; Grb2, growth factor receptor binder 2; ITC, isothermal titration calorimetry; LAT, linker for activation of T-cells; LIC, ligation-independent cloning; MAP, mitogen-activated protein; MAPK, mitogen-activated protein kinase; MD, molecular dynamics; MM, molecular modeling; PDGF, platelet-derived growth factor; PPII, polyproline type II; PR, proline-rich; RTK, receptor tyrosine kinase; SEC, size-exclusion chromatography; SH2, Src homology 2; SH3, Src homology 3; SLS, static light scattering; Sos1, son of sevenless 1*

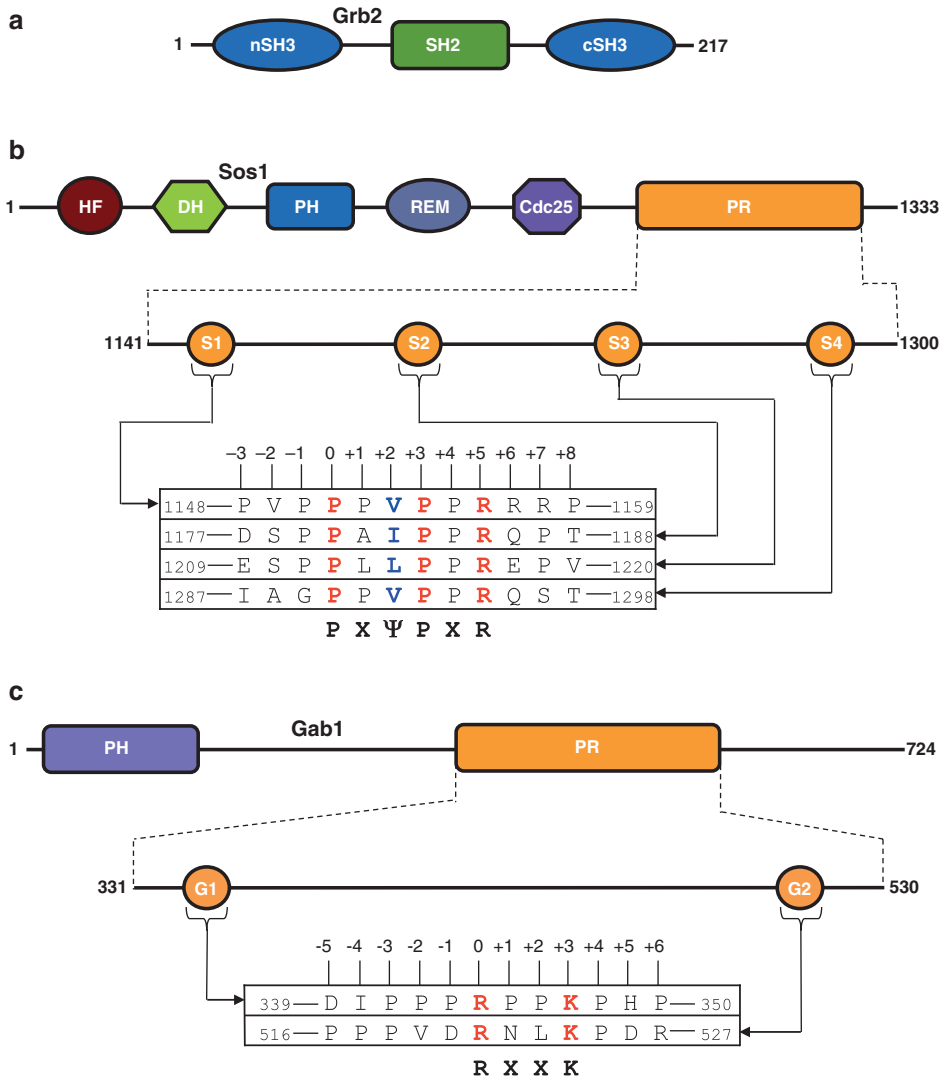

Figure 1. An overview of the various protein constructs used in this study. (a) Grb2 is composed of a central Src homology 2 (SH2) domain flanked between an N-terminal SH3 (nSH3) domain and a C-terminal SH3 (cSH3) domain. (b) Within Sos1, the proline-rich (PR) domain lies at the extreme C-terminal end and contains four distinct PXψPXR motifs, designated S1, S2, S3, and S4. The complete sequences of these four sites are shown. The position of various residues relative to the first proline within the PXψPXR motif, which is designated zero, is indicated. Other domains within Sos1 are HF (histone fold), DH (Dbl homology), PH (pleckstrin homology), REM (Ras exchange motif), and Cdc25. (c) Gab1 is constructed on an N-terminal PH domain and a C-terminal PR domain separated by a long stretch of uncharacterized region. The PR domain contains two distinct RXXK motifs, designated G1 and G2. The amino acid sequence of these motifs and flanking residues within Gab1 is provided. The numbering of various residues within and flanking the RXXK motifs is based on the nomenclature suggested by Feller and co-workers (Harkiolaki *et al*., 2009).

established that the formation of both the Grb2–Sos1 and Grb2–Gab1 complexes is mediated by multivalent interactions (McDonald *et al*., 2012a; McDonald *et al*., 2012b). This scenario is in part made possible by the fact that the PR domains within both Sos1 and Gab1 contain multiple motifs for binding to their respective SH3 domains of Grb2 (Figures 1b and 1c). Thus, while the PR domain of Sos1 contains four distinct PXψPXR motifs (designated S1, S2, S3, and S4) for binding to the nSH3 domain of Grb2, the PR domain of Gab1 bolsters two distinct RXXK motifs (designated G1 and G2) for the recognition of the cSH3 domain of Grb2. Added to this complex design of these PR ligands is also the fact that Grb2 itself exists in a dimer–monomer equilibrium in solution (McDonald *et al*., 2008c). Consistent with these observations, we have also recently shown that although the formation of both Grb2–Gab1 and Grb2–Sos1 complexes occurs with a 2:1 stoichiometry, only the latter is accompanied by positive cooperativity (McDonald *et al*., 2012a; McDonald *et al*., 2012b). Furthermore, while the formation of the Grb2–Gab1 complex is mediated by the binding of both RXXK motifs within Gab1 to the cSH3 domains within Grb2 homodimer, the formation of Grb2–Sos1 appears to be driven by the association of Grb2 homodimer via its nSH3 domains to only two out of four possible PXψPXR motifs within Sos1 at any one time. This implies that the Grb2–Sos1 complex is likely to be conformationally heterogeneous.

Strikingly, the fact that Grb2 contains non-overlapping sites for the binding of Sos1 and Gab1 strongly argues that the recruitment of both of these downstream partners by Grb2 may occur in a non-competitive manner as previously observed within live mammalian cells (Ong *et al*., 2001). This notion was further vindicated by our biophysical analysis showing that peptides containing PXψPXR and RXXK motifs did not compete with

each other for binding to Grb2, leading to the formation of a Sos1–Grb2–Gab1 ternary signaling complex in a non-competitive fashion (McDonald *et al.*, 2010). One major limitation of this latter study was the assumption that the peptides containing PXψPXR and RXXK motifs faithfully mimicked the corresponding intact Sos1 and Gab1 ligands. However, in light of our recent studies (McDonald *et al.*, 2012a; McDonald *et al.*, 2012b), it seems that the PXψPXR and RXXK motifs in the context of intact proteins may behave in a differential manner than in the context of short peptides due to steric hindrance and allosteric factors. In an effort to resolve this central dogma and re-evaluate whether the binding of Sos1 and Gab1 generates two separate Grb2–Sos1 and Grb2–Gab1 pools or favors the formation of a Grb2–Sos1–Gab1 ternary complex, we undertook the current study. Using various biophysical tools, we demonstrate that although Sos1 nucleotide exchange factor and Gab1 docking protein recognize two non-overlapping sites within the Grb2 adaptor, allostery promotes the formation of two physically distinct Grb2–Sos1 and Grb2–Gab1 binary signaling complexes in concert in lieu of a composite Sos1–Grb2–Gab1 ternary complex. In particular, our data reveal that the binding of Sos1 to the nSH3 domain within Grb2 sterically blocks the binding of Gab1 to the cSH3 domain and vice versa in a mutually exclusive manner. Importantly, the formation of both the Grb2–Sos1 and Grb2–Gab1 binary complexes is governed by a stoichiometry of 2:1, in agreement with our previous reports (McDonald *et al.*, 2012a; McDonald *et al.*, 2012b), whereby the respective SH3 domains within Grb2 homodimer bind to Sos1 and Gab1 via multivalent interactions. Collectively, our study sheds new light on the role of allostery in mediating cellular signaling machinery.

MATERIALS AND METHODS

Sample preparation

Full-length human Grb2 (residues 1–217), the PR domain (residues 1141–1300) of human Sos1, and the PR domain (residues 331–530) of human Gab1 were cloned into pET30 bacterial expression vectors with an N-terminal His-tag using Novagen LIC technology. For simplicity, the PR domains of Sos1 and Gab1 will be respectively hereinafter referred to as Sos1_PR and Gab1_PR. All recombinant constructs were expressed in *Escherichia coli* BL21* (DE3) bacterial strain and purified on a Ni-NTA affinity column using standard procedures as described previously (McDonald *et al.*, 2012a; McDonald *et al.*, 2012b). Final yields were typically between 10 and 20 mg protein of apparent homogeneity per liter of bacterial culture. Protein concentration was determined by the fluorescence-based Quant-It assay (Invitrogen) and spectrophotometrically on the basis of extinction coefficients calculated for each recombinant construct using the online software ProtParam at ExPasy Server (Gasteiger *et al.*, 2005). Results from both methods were in excellent agreement. The 12-mer peptides, hereinafter referred to as Sos1_S1 and Gab1_G2 peptides, were derived from the PXψPXR and RXXK motifs corresponding to the S1 and G2 sites within Sos1 and Gab1, respectively (Figures 1b and 1c). Both peptides were commercially obtained from GenScript Corporation. The concentration of peptides was measured gravimetrically.

Isothermal titration calorimetry

Isothermal titration calorimetry (ITC) measurements were performed on a Microcal VP-ITC instrument. Briefly, protein samples were prepared in 50 mM Tris, 200 mM NaCl, 1 mM EDTA, and 5 mM β-mercaptoethanol at pH 8.0. The experiments were initiated by injecting 25 × 10-μl aliquots of 0.5–1 mM of each PR domain from the syringe into the calorimetric cell containing 1.8 ml of 50–100 μM of Grb2 alone or pre-equilibrated with an excess of competing ligand at a molar ratio of 1:5 at various temperatures in the 15–35 °C range. The change in thermal power as a function of each injection was automatically recorded using the ORIGIN software, and the raw data were further processed to yield binding isotherms of heat release per injection as a function of molar ratio of each PR domain to full-length Grb2. The heats of mixing and dilution were subtracted from the heat of binding per injection by carrying out a control experiment in which the same buffer in the calorimetric cell was titrated against each PR domain in an identical manner. The molar ratio (m), the apparent equilibrium dissociation constant (K_d), and the enthalpic change (ΔH) associated with the binding of Grb2 to each PR domain at each temperature were determined with non-linear least-squares fit of data to a one-site binding model as described previously (Wiseman *et al.*, 1989; McDonald *et al.*, 2012a; McDonald *et al.*, 2012b). The binding free energy change (ΔG) was calculated from the following expression:

$$\Delta G = 2RT \ln K_d \quad (1)$$

where the prefix "2" accounts for the bivalent binding of each PR domain to Grb2, R is the universal molar gas constant (1.99 cal/K/mol), and T is the absolute temperature. The entropic contribution ($T\Delta S$) to the free energy of binding was calculated from the relationship:

$$T\Delta S = \Delta H - \Delta G \quad (2)$$

where ΔH and ΔG are as defined above. Heat capacity change (ΔC_p) and enthalpy change at 60 °C (ΔH_{60}) associated with ligand binding to Grb2 were determined from the slopes and y-extrapolations to a temperature of 60 °C of ΔH-T plots, respectively. Changes in solvent-accessible surface area (SASA) upon the binding of various ligands to Grb2 were subsequently calculated from the experimentally determined values of ΔC_p and ΔH_{60}. To determine changes in polar SASA ($\Delta SASA_{polar}$) and apolar SASA ($\Delta SASA_{apolar}$) upon ligand binding to Grb2, it was assumed that ΔC_p and ΔH_{60} are additive and linearly depend on the change in $\Delta SASA_{polar}$ and $\Delta SASA_{apolar}$ as embodied in the following empirically derived expressions (Murphy and Freire, 1992; Spolar and M.T. Record, 1994; Xie and Freire, 1994; Edgcomb and Murphy, 2000):

$$\Delta C_p = a\left[\Delta SASA_{polar}\right] + b\left[\Delta SASA_{apolar}\right] \quad (3)$$

$$\Delta H_{60} = c\left[\Delta SASA_{polar}\right] + d\left[\Delta SASA_{apolar}\right] \quad (4)$$

where a, b, c, and d are empirically determined coefficients with values of −0.14 cal/mol/K/Å^2, +0.32 cal/mol/K/Å^2, +31.34 cal/mol/Å^2, and −8.44 cal/mol/Å^2, respectively. The coefficients a and b are independent of temperature, while c and d refer to a temperature of 60 °C, which equates to the median melting temperature of the proteins from which these constants are derived (Murphy and Freire, 1992; Xie and Freire, 1994; Edgcomb and Murphy, 2000). With ΔC_p and ΔH_{60} experimentally determined using ITC and the knowledge of coefficients a–d from empirical models (Murphy and Freire, 1992; Spolar and M.T. Record, 1994; Xie and Freire, 1994; Edgcomb and Murphy, 2000), Equations (3) and (4) were

simultaneously solved to obtain the magnitudes of $\Delta SASA_{polar}$ and $\Delta SASA_{apolar}$. Total change in SASA ($\Delta SASA_{total}$) is defined by the following equation:

$$\Delta SASA_{total} = \Delta SASA_{polar} + \Delta SASA_{apolar} \quad (5)$$

Molecular modeling

Molecular modeling (MM) was employed to construct a structural model of a ternary complex between Grb2 homodimer bound to the Sos1_PR and Gab1_PR domains using the MODELLER software based on homology modeling (Marti-Renom *et al*., 2000). Briefly, the structural model of this ternary complex was built using structural models of binary complexes between Grb2 homodimer bound to the Sos1_PR and Gab1_PR domains individually as templates as described previously. The structural models of these binary complexes were built on the basis of known crystal or solution structures of Grb2 homodimer (PDB# 1GRI), the nSH3 domain of Grb2 bound to PXψPXR motifs (PDB# 4GBQ), and the cSH3 domain of Grb2 bound to RXXK motifs (PDB# 2W0Z/2VWF) as fully described earlier (McDonald *et al*., 2012a; McDonald *et al*., 2012b). Additionally, the Sos1_PR and Gab1_PR domains were folded into compact globular-like topologies using the QUARK server based on *ab initio* modeling. The QUARK server can be accessed online at http://zhanglab.ccmb.med.umich.edu/quark. It should be noted that the structural model of Grb2 in complex with the Sos1_PR domain was based on a bivalent interaction between the nSH3 domains of Grb2 homodimer and the S1/S4 sites within the Sos1_PR domain, while that of Grb2 bound to the Gab1_PR domain was based on a bivalent interaction between the cSH3 domains of Grb2 homodimer and the G1/G2 sites within the Gab1_PR domain as described previously (McDonald *et al*., 2012a; McDonald *et al*., 2012b). A total of 100 structural models were calculated, and the structure with the lowest energy, as judged by the MODELLER Objective Function, was selected for further analysis. The modeled structure was rendered using RIBBONS (Carson, 1991). All calculations and data processing were performed on a Linux workstation equipped with a dual-core processor.

Molecular dynamics

Molecular dynamics (MD) simulations were performed with GROMACS (Van Der Spoel *et al*., 2005; Hess, 2008) using the integrated OPLS-AA force field (Jorgensen and Tirado-Rives, 1988; Kaminski *et al*., 2001). Briefly, the modeled structure of a ternary complex between Grb2 homodimer bound to the Sos1_PR and Gab1_PR domains was centered within a cubic box and hydrated using the extended simple point charge (SPC/E) water model (Toukan and Rahman, 1985; Berendsen *et al*., 1987). The hydrated structures were energy-minimized with the steepest descent algorithm prior to equilibration under the NPT ensemble conditions, wherein the number of atoms (N), pressure (P) and temperature (T) within the system were respectively kept constant at ~10^5, 1 bar and 300 K. The Particle-Mesh Ewald (PME) method was employed to compute long-range electrostatic interactions with a 10 Å cut-off (Darden *et al*., 1993) and the Linear Constraint Solver (LINCS) algorithm to restrain bond lengths (Hess *et al*., 1997). All MD simulations were performed under periodic boundary conditions (PBC) using the leapfrog integrator with a time step of 2 fsec. For the final MD production runs, data were collected every 10 psec over a time scale of 100 nsec. All MD simulations were run on a Linux workstation using parallel processors at the High Performance Computing facility within the Center for Computational Science of the University of Miami.

RESULTS AND DISCUSSION

Sos1 competes with Gab1 for binding to Grb2 and vice versa

In a previous development (McDonald *et al*., 2010), we demonstrated that peptides derived from Sos1 and Gab1, containing PXψPXR and RXXK motifs, did not compete with each other for binding to Grb2 such that that the formation of the Sos1–Grb2–Gab1 ternary signaling complex occurred in a non-competitive fashion. It is telling that this previous study suffered from one drawback in that the short peptides containing PXψPXR and RXXK motifs were assumed to faithfully mimic the intact Sos1 and Gab1 proteins. However, in light of our recent studies (McDonald *et al*., 2012a; McDonald *et al*., 2012b), it seems that the PXψPXR and RXXK motifs in the context of intact proteins may behave in a differential manner than in the context of short peptides due to steric hindrance and allosteric modulation. In an attempt to test this hypothesis, we measured the binding of the PR domains of Sos1 (Sos1_PR) and Gab1 (Gab1_PR) to full-length Grb2 alone and in the presence of each other using ITC. Additionally, we also analyzed the binding of these PR domains to Grb2 pre-equilibrated with 12-mer peptides derived from the S1 site in Sos1 (Sos1_S1) and G2 site in Gab1 (Gab1_G2). The Sos1_S1 and Gab1_G2 peptides were chosen because they bind to Grb2 with highest affinities compared with peptides derived from other sites in Sos1 and Gab1 (McDonald *et al*., 2008a; McDonald *et al*., 2009b; McDonald *et al*., 2011). Representative ITC data obtained from these measurements are shown in Figures 2 and 3, while the corresponding thermodynamic parameters derived from the fit of these data to a one-site binding model are reported in Tables 1 and 2. It is noteworthy that although the binding of the Sos1_PR and Gab1_PR domains to full-length Grb2 alone has been reported previously (McDonald *et al*., 2012a; McDonald *et al*., 2012b), it was necessary to conduct these measurements again here in order to directly compare how the presence of one PR domain would affect the binding of the other to Grb2. For the same reason, we also carried out ITC analysis for the binding of Sos1_S1 and Gab1_G2 peptides to full-length Grb2 again even though it has been reported earlier (McDonald *et al*., 2010).

Importantly, we would also like to mention that although we have not been successful in the purification of full-length Sos1 (153kD) and Gab1 (77kD) proteins because of insurmountable technical hurdles, the Sos1_PR (17kD) and Gab1_PR (22kD) domains should nonetheless suffice as better mimetics of intact proteins in lieu of short peptides. Notwithstanding these limitations, our data provide striking insights into the molecular mechanism of binding of Sos1 and Gab1 to Grb2 in concert. Notably, the Sos1_PR domain binds to Grb2 with a 2:1 stoichiometry (Table 1), implying that the Grb2–Sos1 interaction is most likely driven by the binding of both nSH3 domains within Grb2 homodimer to two out of four possible PXψPXR motifs within Sos1 in a bivalent manner as described recently (McDonald *et al*., 2012a). When Grb2 is pre-equilibrated with the Gab1_PR domain, the latter inhibits the binding of the Sos1_PR domain to Grb2 by more than fivefold (Table 1). Given that Grb2 primarily recognizes PXψPXR motifs within Sos1 through its nSH3 domain

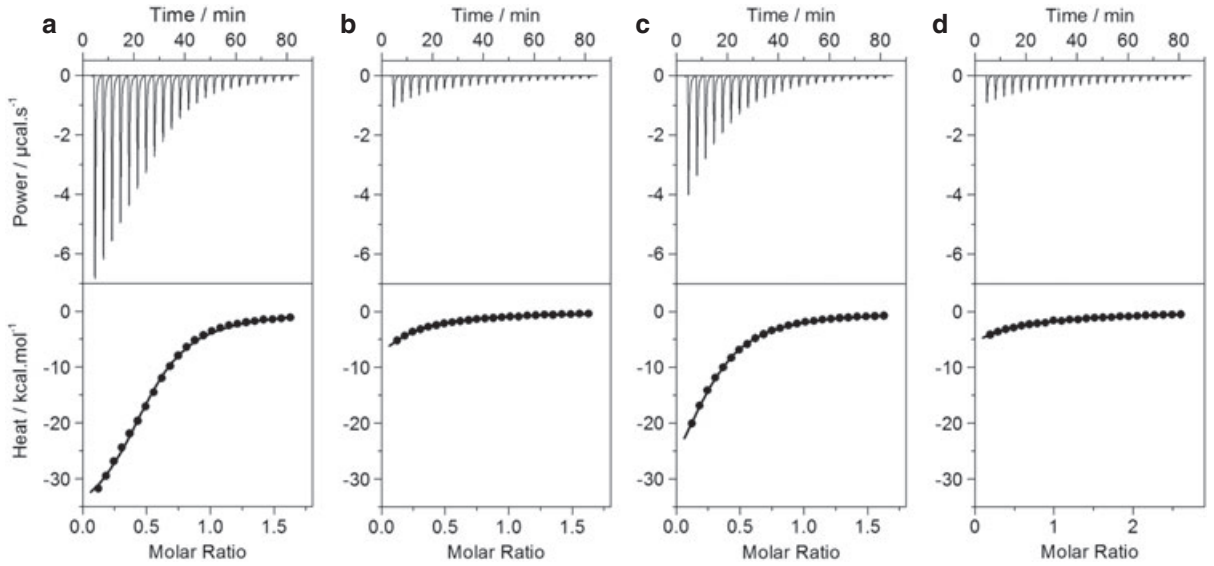

Figure 2. ITC analysis of the binding of Sos1_PR domain to Grb2 alone (a), Grb2 pre-equilibrated with Gab1_PR domain (b), Grb2 pre-equilibrated with Gab1_G2 peptide (c), and Grb2 pre-equilibrated with Sos1_S1 peptide (d). The upper panels show raw ITC data expressed as change in thermal power with respect to time over the period of titration. In the lower panels, change in molar heat is expressed as a function of molar ratio of Sos1_PR domain to Grb2. The solid lines in the lower panels show the fit of data to a one-site binding model, as described previously (Wiseman *et al*., 1989; McDonald *et al*., 2012a; McDonald *et al*., 2012b), using the ORIGIN software.

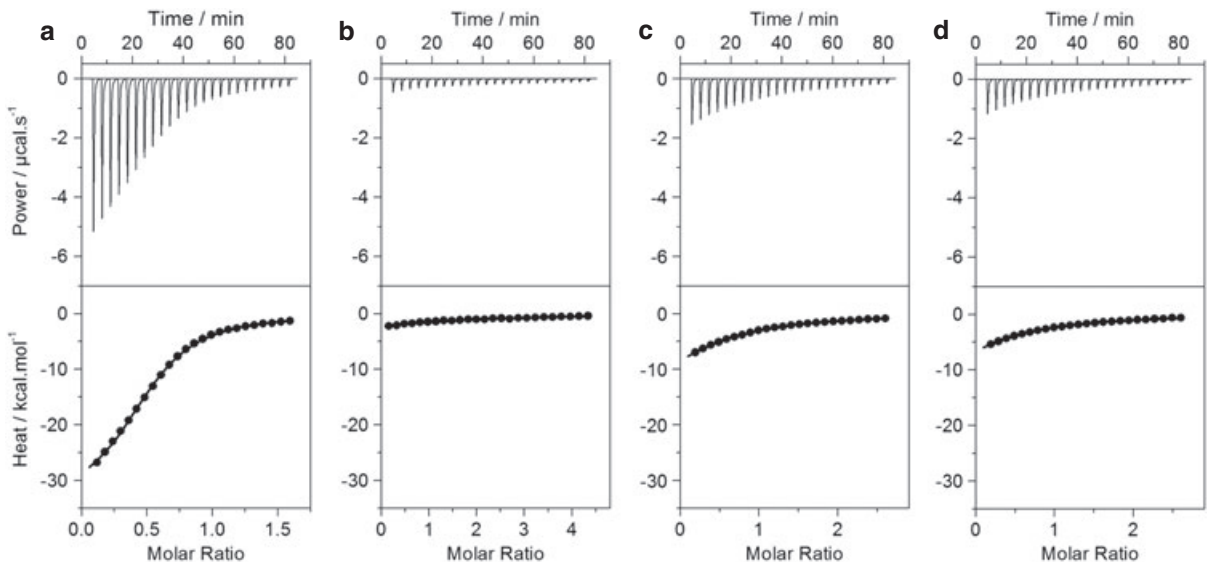

Figure 3. ITC analysis of the binding of Gab1_PR domain to Grb2 alone (a), Grb2 pre-equilibrated with Sos1_PR domain (b), Grb2 pre-equilibrated with Sos1_S1 peptide (c), and Grb2 pre-equilibrated with Gab1_G2 peptide (d). The upper panels show raw ITC data expressed as change in thermal power with respect to time over the period of titration. In the lower panels, change in molar heat is expressed as a function of molar ratio of Gab1_PR domain to Grb2. The solid lines in the lower panels show the fit of data to a one-site binding model, as described previously (Wiseman *et al*., 1989; McDonald *et al*., 2012a; McDonald *et al*., 2012b), using the ORIGIN software.

(McDonald *et al*., 2010; McDonald *et al*., 2012a), while the Grb2–Gab1 interaction is exclusively mediated by the binding of the cSH3 domain of Grb2 to RXXK motifs within Gab1 (Lock *et al*., 2000; Lewitzky *et al*., 2001; McDonald *et al*., 2011; McDonald *et al*., 2012b), the most straightforward interpretation of this salient observation is that the Gab1_PR domain sterically hinders the binding of Sos1_PR to Grb2 in lieu of direct competition for the putative ligand binding sites.

Ironically, our data further suggest that not only the Gab1_PR domain but also the Gab1_G2 peptide reduces the binding affinity of the Sos1_PR domain to Grb2, albeit to a much lesser extent (Table 1). In light of the fact that the much shorter peptide docked at the cSH3 domain within Grb2 is unlikely to sterically hinder the binding of the Sos1_PR domain to the neighboring nSH3 domain, we argue that the ability of Gab1 to restrict the binding of Sos1 to Grb2 not only resides in steric hindrance but also may be due to its ability to cause a subtle conformational change within Grb2 upon binding to the cSH3 domain. This conformational change may be transmitted to the nSH3 domain through an allosteric communication channel such that

Table 1. Thermodynamic parameters obtained from ITC measurements for the binding of the Sos1_PR domain to Grb2 alone and pre-equilibrated with various ligands

	m	*n*	K_d (μM)	ΔH (kcal.mol^{-1})	$T\Delta S$ (kcal.mol^{-1})	ΔG (kcal.mol^{-1})
Grb2 alone	2.08 ± 0.08	2:1	6.83 ± 0.30	−39.56 ± 0.69	−25.45 ± 0.74	−14.11 ± 0.05
Grb2 + Gab1_PR	10.77 ± 0.78	11:1	38.69 ± 0.74	−40.18 ± 0.17	−28.13 ± 0.15	−12.05 ± 0.02
Grb2 + Gab1_G2	3.70 ± 0.04	4:1	14.19 ± 0.56	−39.29 ± 0.35	−26.05 ± 0.31	−13.24 ± 0.05
Grb2 + Sos1_S1	6.91 ± 1.36	7:1	56.13 ± 6.86	−40.45 ± 0.73	−28.83 ± 0.87	−11.61 ± 0.15

Note that *m* is the molar ratio of Grb2 bound to the Sos1_PR domain directly calculated from non-linear least-squares fit of ITC data to a one-site binding model as described previously (Wiseman *et al*., 1989; McDonald *et al*., 2012a; McDonald *et al*., 2012b), while *n* is the corresponding stoichiometry observed for the binding of Grb2 to Sos1 to the nearest integer. Errors were calculated from at least three independent measurements. All errors are given to one standard deviation.

Table 2. Thermodynamic parameters obtained from ITC measurements for the binding of the Gab1_PR domain to Grb2 alone and pre-equilibrated with various ligands

	m	*n*	K_d (μM)	ΔH (kcal.mol^{-1})	$T\Delta S$ (kcal.mol^{-1})	ΔG (kcal.mol^{-1})
Grb2 alone	1.96 ± 0.01	2:1	7.58 ± 0.01	−34.30 ± 0.31	−20.32 ± 0.31	−13.98 ± 0.01
Grb2 + Sos1_PR	2.06 ± 0.09	2:1	105.54 ± 3.46	−19.07 ± 0.52	−8.21 ± 0.48	−10.86 ± 0.04
Grb2 + Sos1_S1	1.99 ± 0.01	2:1	43.39 ± 0.66	−21.45 ± 0.52	−9.54 ± 0.51	−11.91 ± 0.02
Grb2 + Gab1_G2	2.02 ± 0.09	2:1	42.92 ± 0.52	−16.81 ± 0.11	−4.88 ± 0.10	−11.93 ± 0.01

Note that *m* is the molar ratio of Grb2 bound to the Gab1_PR domain directly calculated from non-linear least-squares fit of ITC data to a one-site binding model as described previously (Wiseman *et al*., 1989; McDonald *et al*., 2012a; McDonald *et al*., 2012b), while *n* is the corresponding stoichiometry observed for the binding of Grb2 to Gab1 to the nearest integer. Errors were calculated from at least three independent measurements. All errors are given to one standard deviation.

the binding groove within the latter becomes somewhat disconfigured so as to compromise its binding to Sos1. These findings are consistent with our earlier report in which we demonstrated that the binding of Sos1_S1 peptide to the nSH3 domain allosterically induces a conformational change within Grb2 so as to allow Gab1_G2 peptide access to the cSH3 domain in an exclusively non-competitive manner to generate the Sos1–Grb2–Gab1 ternary complex (McDonald *et al*., 2010). Importantly, our data also indicate that the Sos1_S1 peptide is a much better competitor of the Sos1_PR domain than both the Gab1_PR domain and Gab1_G2 peptide by virtue of its ability to directly compete with the Sos1_PR domain for binding to the nSH3 domain (Table 1). This finding further lends support to the notion that Gab1 blocks the binding of Sos1 to Grb2 through steric hindrance and allosteric communication in lieu of directly competing for the nSH3 domain within Grb2.

In a manner akin to the binding of the Sos1_PR domain, the Gab1_PR domain also binds to Grb2 with a 2:1 stoichiometry (Table 2), implying that the Grb2–Gab1 interaction is most likely driven by the binding of both cSH3 domains within Grb2 homodimer to both RXXK motifs within Sos1 in a bivalent manner as described recently (McDonald *et al*., 2012b). When Grb2 is pre-equilibrated with the Sos1_PR domain, the latter appears to inhibit the binding of the Gab1_PR domain to Grb2 by more than an order of magnitude (Table 2), implying that Sos1 blocks the binding of Gab1 to Grb2 more effectively than being blocked by Gab1. The fact that not only the Sos1_PR domain but also the Sos1_S1 peptide inhibits the binding of the Gab1_PR domain to Grb2 further cements our thesis that Sos1 and Gab1 bind to Grb2 in a mutually exlusive manner via steric hindrance and allosteric conformational changes so as to alter the structural configuration of the binding grooves within each other's binding sites within Grb2 upon association. Finally, the Gab1_G2 peptide restricts the binding of the Gab1_PR domain to Grb2 although it appears to be a much poorer competitor compared to the Sos1_PR domain (Table 2). This is in remarkable contrast to the fact that the Sos1_S1 peptide is a better competitor of the Sos1_PR domain than the Gab1_PR domain for binding to Grb2 (Table 1). We also note that while the observed binding stoichiometry of the Sos1_PR domain to Grb2 alone is 1:2, it steadily rises to as high as 1:11 in the presence of competing ligands (Table 1). This implies that the competing ligands bind to Grb2 in an apparently irreversible manner and thereby lower the effective concentration of Grb2 available for the incoming Sos1_PR domain. In a remarkable contrast, the observed binding stoichiometry of the Gab1_PR domain to Grb2 alone is 1:2 and does not change in the presence of competing ligands (Table 2), arguing that the competing ligands bind Grb2 in an apparently reversible manner and do not lower the effective concentration of Grb2 available to the incoming Gab1_PR domain. We attribute such discrepancies in the observed binding stoichiometries of the Sos1_PR and Gab1_PR domains to Grb2 alone versus Grb2 pre-equilibrated with competing ligands to their distinct thermodynamic modes of binding. Indeed, while the binding of both the Sos1_PR and Gab_PR domains to Grb2 is under favorable enthalpic changes accompanied by unfavorable entropic contributions to the overall free energy (Table 1 and 2), the precise contributions deserve a closer look. Thus, while enthalpic contribution to the free energy for the binding of the Sos1_PR domain to Grb2 alone and in the presence of competing ligands remains more or less unchanged (Table 1), it is somewhat substantially reduced in the case of the binding of the Gab1_PR domain to Grb2 alone versus Grb2 pre-equilibrated with competing ligands (Table 2).

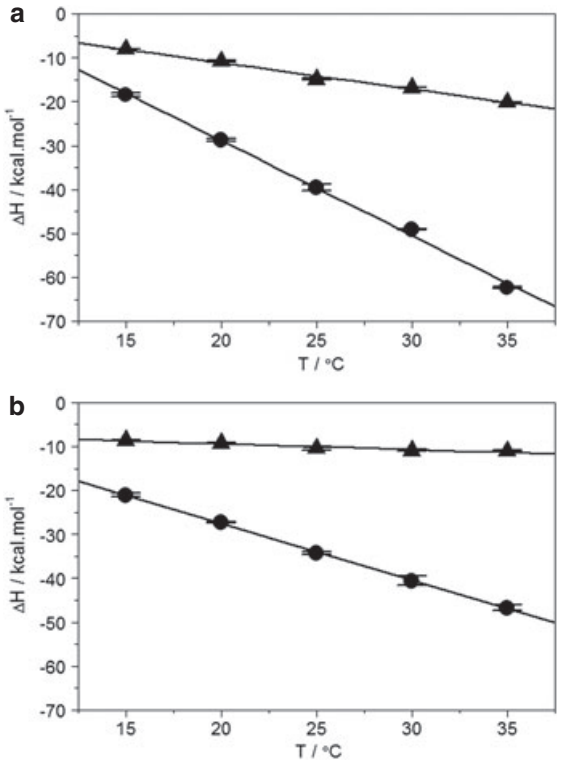

Figure 4. Enthalpy (Δ*H*)–Temperature (*T*) plots for the binding of Grb2 to various ligands. (a) Binding of Grb2 to Sos1_PR domain (●) and Sos1_S1 peptide (▲). (b) Binding of Grb2 to Gab1_PR domain (●) and Gab1_G2 peptide (▲). The solid lines through the data points represent linear fits. Error bars were calculated from at least three independent measurements to one standard deviation.

Binding of Sos1 and Gab1 to Grb2 is associated with substantial conformational changes

Our data presented above unequivocally demonstrate that Sos1 and Gab1 associate with Grb2 in a mutually exclusive manner. We believe that such association is most likely driven through steric hindrance and allosteric conformational changes in lieu of Sos1 and Gab1 competing with each other for the SH3 domains. In an effort to further test the extent of such conformational changes, we next measured and compared heat capacity change (ΔC_p) accompanying ligand binding to Grb2 (Figure 4). As shown in Table 3, our data reveal that although ΔC_p associated with the binding of various ligands to Grb2 is negative, its magnitude varies substantially depending on the nature of ligand. It is telling that ΔC_p associated with the binding of the Sos1_PR domain to Grb2 is more than threefold greater than that observed for the binding of the Sos1_S1 peptide, while ΔC_p associated with the binding of the Gab1_PR domain to Grb2 is more than an order of magnitude larger relative to the binding of the Gab1_G2 peptide. It should be noted that while the binding of above-mentioned ligands to Grb2 has been described previously (McDonald *et al*., 2010; McDonald *et al*., 2012a; McDonald *et al*., 2012b), the temperature-dependence of the enthalpic change associated with their binding is being reported here for the first time.

Importantly, a negative value of ΔC_p implies that the burial of apolar surface dominates intermolecular association over polar groups, and the more negative the value of ΔC_p, the greater the extent of such burial of apolar surface. In fact, semi-empirical relationships have been developed to quantify the extent of change in solvent-accessible surface area (ΔSASA) from experimentally determined values of ΔC_p for intermolecular associations (Murphy and Freire, 1992; Freire, 1993; Spolar and M.T. Record, 1994; Xie and Freire, 1994; Murphy, 1999; Edgcomb and Murphy, 2000). Taking advantage of these relationships, we also determined and compared the extent of burial of apolar and polar surfaces upon ligand binding to Grb2 (Table 3). Consistent with our data above, our ΔSASA calculations suggest that the binding of the Sos1_PR and Gab1_PR domains to Grb2 results in much greater burial of apolar surfaces compared to the binding of the Sos1_S1 and Gab1_G2 peptides. These data thus further corroborate the notion that the binding of Sos1_PR and Gab1_PR to Grb2 is accompanied by substantial conformational changes within Grb2 and/or the PR domains. Notably, such conformational ordering may underscore the physical basis of the formation of two distinct Grb2–Sos1 and Grb2–Gab1 binary complexes instead of a composite Sos1–Grb2–Gab1 ternary complex through steric hindrance and allosteric modulation.

Structural basis of the formation of two distinct Grb2–Sos1 and Grb2–Gab1 binary complexes instead of a composite Sos1–Grb2–Gab1 ternary complex

Proline-rich sequences in proteins not only play a central role in mediating cellular signaling cascades pertinent to health and disease but also constitute a major component of human proteome. Despite their important roles, our knowledge of 3D conformations adopted by PR proteins remains poor due largely to the fact that they are not amenable to structural analysis at the atomic level by conventional methods such as x-ray crystallography and nuclear magnetic resonance. This limitation arises because PR proteins are structurally flexible due to the rigidity of proline sidechain as well as being largely deficient in secondary structural elements such as α-helices and β-strands that constitute the bedrock of αβ proteins with a well-defined

Table 3. ΔSASA values determined from thermodynamic parameters for the binding of various ligands to Grb2 alone

	ΔH_{60} (kcal.mol^{-1})	ΔC_p (kcal.mol^{-1}.K^{-1})	$\Delta SASA_{polar}$ (Å^2)	$\Delta SASA_{apolar}$ (Å^2)	$\Delta SASA_{total}$ (Å^2)
Sos1_PR	-115.30 ± 0.93	−2.16 ± 0.03	−6236 ± 2	−9494 ± 110	−15 731 ± 106
Gab1_PR	−79.31 ± 1.39	−1.29 ± 0.03	−4104 ± 85	−5843 ± 148	−9946 ± 232
Sos1_S1	−35.23 ± 0.27	−0.60 ± 0.01	−1846 ± 23	−2683 ± 54	−4528 ± 78
Gab1_G2	−14.60 ± 0.05	−0.13 ± 0.01	−646 ± 9	−674 ± 26	−1319 ± 35

Errors were calculated from at least three independent measurements. All errors are given to one standard deviation.

structure. Because of these limitations, we employed here MM as an alternative to unearth the physical basis of the formation of two distinct Grb2–Sos1 and Grb2–Gab1 binary complexes instead of a composite Sos1–Grb2–Gab1 ternary complex through steric hindrance and allosteric modulation. Accordingly, in agreement with our previous studies (McDonald *et al*., 2012a; McDonald *et al*., 2012b), we modeled the structure of a ternary complex between Grb2 homodimer bound to the Sos1_PR and Gab1_PR domains so as to shed light on how the binding of one ligand may hinder the binding of the other and vice versa (Figure 5). In this structural model, the Grb2–Sos1 interaction is mediated by the bivalent binding of Grb2 homodimer via its nSH3 domains to the two PXψPXR motifs located within the S1/S4 sites in Sos1_PR, while the bivalent binding of Grb2 homodimer via its cSH3 domains to two RXXK motifs located within the G1 and G4 sites in Gab1_PR accounts for the Grb2–Gab1 interaction as described earlier (McDonald *et al*., 2012a; McDonald *et al*., 2012b). It is noteworthy that the monomers within Grb2 homodimer adopt a twofold axis of symmetry such that the SH2 domain of one monomer docks against the cSH3 domain of the other and vice versa in a head-to-tail fashion as observed in the crystal structure determined by Ducruix and co-workers (Maignan *et al*., 1995).

Importantly, our structural modeling reveals molecular insights into the binding of the Sos1_PR and Gab1_PR domains to Grb2. In the case of the binding of the Sos1_PR domain to Grb2, each PXψPXR motif located within the S1/S4 sites latches onto the hydrophobic groove running parallel to the RT loop within the β-barrel fold of each nSH3 domain and adopts a left-handed polyproline type II (PPII)–helical conformation in a canonical fashion (Goudreau *et al*., 1994; Terasawa *et al*., 1994; Wittekind *et al*., 1994; Wittekind *et al*., 1997). Within each nSH3 hydrophobic groove, the PXψPXR motifs are stabilized by an extensive network of intermolecular contacts as reported earlier (McDonald *et al*., 2008b; McDonald *et al*., 2009a; McDonald *et al*., 2010; McDonald *et al*., 2012a). Notably, the binding of the Sos1_PR domain to Grb2 shares both similarities and differences with the binding of the Gab1_PR domain. Thus, while PXψPXR

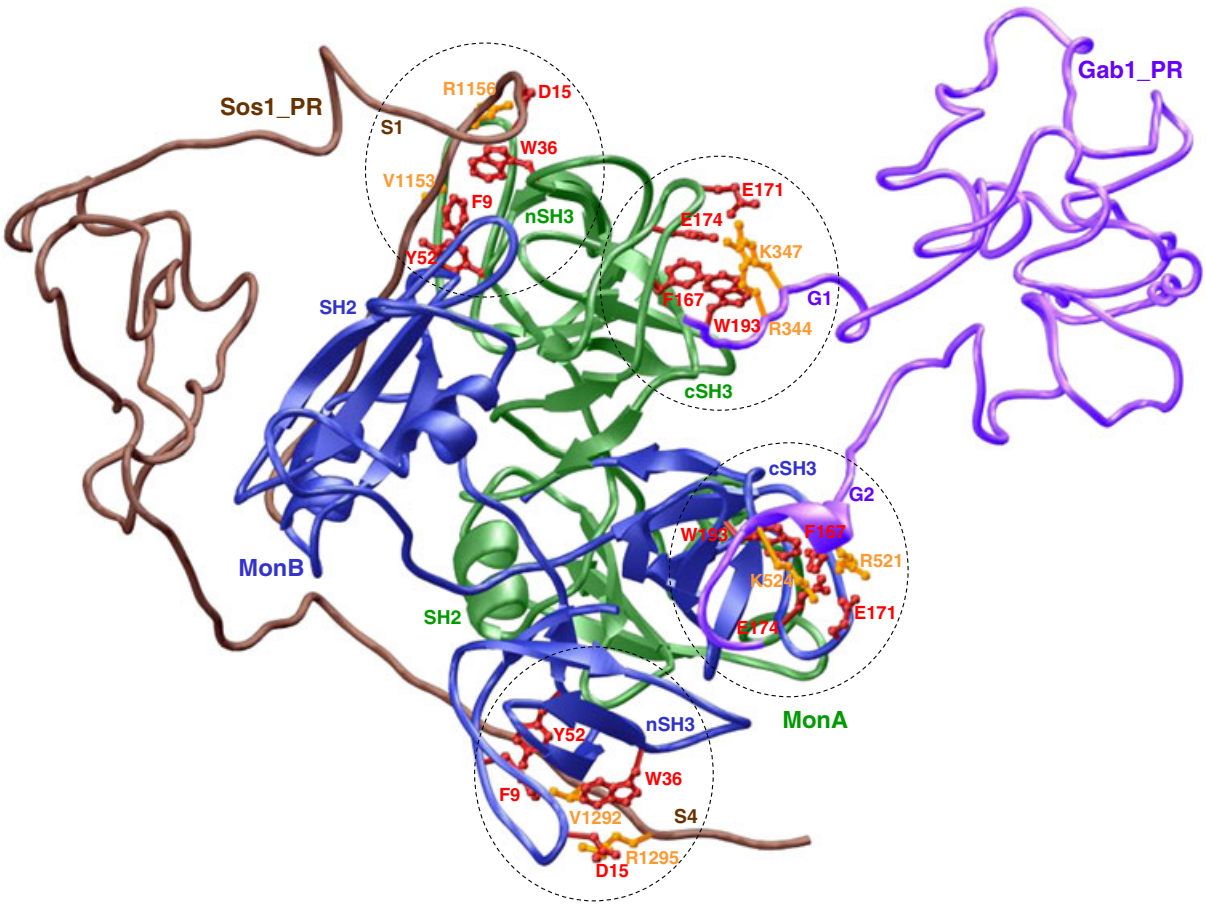

Figure 5. Structural model of Grb2 bound to the PR domains of Sos1 (Sos1_PR) and Gab1 (Gab1_PR) in the context of a Sos1–Grb2–Gab1 ternary complex. Note that within this ternary complex, the Grb2–Sos1 interaction is mediated via the binding of nSH3 domains of Grb2 homodimer to PXψPXR motifs located at S1/S4 sites within Sos1, while the Grb2–Gab1 interaction is driven via the binding of cSH3 domains of Grb2 homodimer to RXXK motifs located at G1/G2 sites within Gab1. One monomer of Grb2 is shown in green (MonA) and the other in blue (MonB). Sos1_PR is colored brown, while Gab1_PR is shown in magenta. For clarity, the Grb2–Sos1 and Grb2–Gab1 interfaces between the hydrophobic grooves within the respective SH3 domains of Grb2 monomers accommodating the corresponding PXψPXR or RXXK motifs are marked by dashed circles. The sidechain moieties of ψ and arginine residues within the PXψPXR motifs at S1/S4 sites and the sidechain moieties of arginine and lysine residues within the RXXK motifs at G1/G2 sites are colored yellow. The sidechain moieties of residues within the nSH3 domains of Grb2 that interact with ψ and arginine residues within the PXψPXR motifs and the sidechain moieties of residues within the cSH3 domains of Grb2 that interact with arginine and lysine residues within the RXXK motifs are colored red.

and RXXK motifs within both the Sos1_PR and Gab1_PR domains recognize the analogous binding grooves within both the nSH3 and cSH3 domains, they do so via distinct mechanisms. For example, while the S1/S4 motifs within Sos1_PR bind to the nSH3 domains in a similar manner, the G1/G2 motifs within the Gab1_PR domain recognize the cSH3 domains in distinct manners as reported previously (McDonald *et al*., 2011). Thus, while the G1 motif strictly requires the PPRPPKP consensus sequence for high-affinity binding to the cSH3 domain, the G2 motif displays preference for the PXVXRXLKPXR consensus. Although both G1 and G2 motifs are accommodated within the same hydrophobic groove located within the β-barrel fold of each cSH3 domain, there are some notable differences in their modes of binding. Thus, while the G1 motif adopts the relatively open PPII-helical conformation upon binding to the cSH3 domain, the G2 motif assumes a much tighter 3_{10}-helical conformation. Remarkably, despite such distinguishing conformations, the nature of residues within each cSH3 domain involved in interacting with G1 and G2 motifs bear substantial similarities and engage in an intricate network of intermolecular contacts with their counterparts lining the hydrophobic groove within each cSH3 domain in stabilizing these key SH3-ligand interactions as fully discussed earlier (McDonald *et al*., 2011; McDonald *et al*., 2012b).

We add that although the spatial orientations of PXψPXR and RXXK motifs relative to their respective SH3 domains within Grb2 homodimer can be relied upon with a high degree of confidence at the atomic level, due to the fact that they were modeled on the basis of high sequence identity with corresponding templates, there is a high probability of uncertainty in the relative orientation and conformation of the intervening polypeptide chains spanning the S1/S4 or G1/G2 sites within the PR domains. Notably, these intervening polypeptide chains were folded into a compact globular-like topology on the basis of *ab initio* modeling without any template. Our previous studies revealed that the Sos1_PR and Gab1_PR domains represent structurally disordered regions devoid of a well-defined compact fold (McDonald *et al*., 2012a; McDonald *et al*., 2012b). We believe that these intervening polypeptide chains are conformationally flexible within both the Sos1_PR and Gab1_PR domains, and thus, the binding of one to Grb2 may sterically hinder the binding of the other in a mutually exclusive manner. This is further supported by our structural model in that the nSH3 and cSH3 domains are juxtaposed to each other within each monomer of Grb2 homodimer, arguing that ligand binding to the nSH3 domain may restrict access to another ligand binding to the cSH3 domain and vice versa. Accordingly, such steric hindrance may favor the formation of two distinct Grb2–Sos1 and Grb2–Gab1 binary complexes instead of a composite Sos1–Grb2–Gab1 ternary complex as suggested by our thermodynamic data.

It is also noteworthy that the relative orientation of monomers within Grb2 homodimer places the nSH3 domains within each monomer on one face of the molecule while the cSH3 domains are on the opposite face. Accordingly, the bivalent sites within Grb2 homodimer for accommodating Sos1 and Gab1 are physically separated. This salient observation argues against the notion that the binding of Sos1 to the nSH3 domains on one face and Gab1 to the cSH3 domains on the opposite face may encounter steric clashes. However, our structural model also reveals that although bivalent sites for accommodating Sos1 and Gab1 are physically separated, there are notable differences in the inter-domain distances. Thus, while a distance of ~25 Å separates one cSH3 domain from the other within Grb2 homodimer, the nSH3 domains are placed apart by ~50 Å. Accordingly, the rather large distance between the two nSH3 domains implies that the intervening polypeptide chain spanning the S1/S4 sites in Sos1 may adopt multiple orientations and that such flexibility may promote steric clashes between Sos1 and Gab1 upon binding to Grb2 in concert. Despite these plausible scenarios as to how the binding of Sos1 to Grb2 may sterically block the binding of Gab1 and vice versa, our structural model does not provide insights into any conformational changes that may be coupled to ligand binding. Thus, it is equally conceivable that the binding of one ligand at one site induces conformational changes within Grb2 such that the binding of the other ligand at the second site is blocked in an allosteric manner.

MD simulations suggest a high probability of steric hindrance between Sos1 and Gab1 within the composite Sos1–Grb2–Gab1 ternary complex

In an attempt to further understand how steric hindrance and allosteric conformational changes upon ligand binding may favor the formation of two distinct Grb2–Sos1 and Grb2–Gab1 binary complexes instead of a composite Sos1–Grb2–Gab1 ternary complex, we next performed MD simulations on the structural model of a ternary complex between Grb2 homodimer bound to the Sos1_PR and Gab1_PR domains (Figure 6). Importantly, we assessed the stability and dynamics of the ternary complex and various constituent components in terms of the root mean square deviation (RMSD) of backbone atoms as a function of simulation time as well as through the superimposition of snapshots of a family of simulated structures recorded at various times along the MD simulation.

As shown in Figure 6a, the MD trajectory reveals that the Sos1–Grb2–Gab1 ternary complex reaches structural equilibrium with an RMSD of ~12 Å after about 20 nsec. To understand the origin of such high structural fluctuations, we deconvoluted the overall RMSD of the ternary complex into its four constituent components: the Sos1_PR and Gab1_PR domains and the Grb2 monomers, designated MonA and MonB. Our analysis reveals that while Grb2 monomers display relatively high stability with an RMSD of ~2 Å over the entire course of MD simulation, the Sos1_PR and Gab1_PR remain relatively unstable with RMSD values exceeding 15 Å and 10 Å, respectively. This strongly argues that the Sos1_PR and Gab1_PR domains are structurally flexible. This is further demonstrated through the superposition of various simulated structures of the Sos1–Grb2–Gab1 ternary complex at 10-nsec time intervals along the MD trajectory (Figure 6b). It is evident from such analysis that although the S1/S4 motifs within the Sos1_PR and G1/G2 motifs within Gab1_PR adopt relatively stable conformations within their respective SH3 grooves, the intervening polypeptide chains spanning these motifs display rather high structural plasticity. Accordingly, such structural flexibility could promote an overlapping of the Sos1_PR and Gab1_PR domains when bound to Grb2 due to conformational dynamics lasting over longer time regimes of micro- or milliseconds, which would be more reflective of bona fide molecular motions of multi-protein complexes relevant to their physiological function. However, studying conformational dynamics of multi-protein complexes over time scales of microseconds, much less milliseconds, is computationally very challenging and currently not a feasible exercise. Importantly, additional physical constraints placed upon the PR

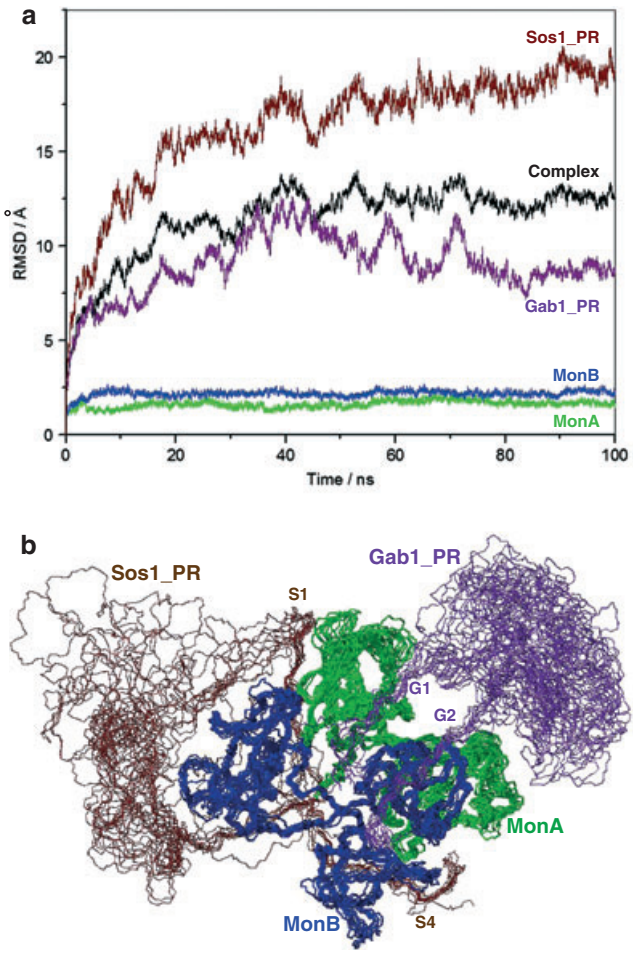

Figure 6. MD analysis on the structural model of Grb2 bound to the PR domains of Sos1 (Sos1_PR) and Gab1 (Gab1_PR) in the context of a Sos1–Grb2–Gab1 ternary complex. (a) Root mean square deviation (RMSD) of backbone atoms (N, Cα, and C) within each simulated structure relative to the initial modeled structure of Sos1–Grb2–Gab1 ternary complex as a function of simulation time. Note that the overall RMSD for the ternary complex (black) is deconvoluted into PR domains of Sos1 (brown) and Gab1 (magenta) and into each of the two Grb2 monomers, designated MonA (green) and MonB (blue). (b) Superimposition of simulated structures of Sos1–Grb2–Gab1 ternary complex obtained at 10-nsec time intervals in the 100-nsec MD trajectory. One monomer of Grb2 is shown in green (MonA) and the other in blue (MonB). Sos1_PR is colored brown, while Gab1_PR is shown in magenta. The S1/S4 motifs within Sos1_PR and G1/G2 motifs within Gab1_PR involved in mediating binding to Grb2 are marked for clarity.

domains in the context of intact Sos1 and Gab1 proteins in complex with Grb2 may also facilitate their physical overlap due to steric clashes with neighboring domains within the binding partners. The same argument would also likely hold true in the context of a live cellular milieu, where molecular crowding and noise due to a plethora of non-specific and promiscuous interactions with other cellular proteins would be expected to physically constrain the conformational space available to the PR domains of Sos1 and Gab1. In short, our MD simulations support the notion that the rather high structural plasticity of the Sos1_PR and Gab1_PR domains combined with other physical constraints in their immediate vicinity may account for their ability to sterically hinder the binding of each other to Grb2.

CONCLUSIONS

Multi-protein complexes play key roles in driving a multitude of cellular signaling cascades central to health and disease. However, our knowledge of how the binding of one ligand affects the overall stoichiometry of a multi-protein complex remains largely obscure. In particular, the role of steric hindrance and allosteric communication in dictating ligand binding to proteins with multiple binding sites remains highly underappreciated. In an effort to understand the assembly of multi-protein complexes, we undertook detailed biophysical analysis on how the binding of Sos1 guanine nucleotide exchange factor to Grb2 adaptor may affect the binding of Gab1 docking protein and vice versa. Given that Sos1 recognizes Grb2 via its nSH3 domain (McDonald *et al*., 2010; McDonald *et al*., 2012a), while Gab1 binds to the cSH3 domain within Grb2 in an exclusive manner (Lock *et al*., 2000; Lewitzky *et al*., 2001; McDonald *et al*., 2012b), one could be forgiven for arguing in favor of the formation of a Sos1–Grb2–Gab1 ternary complex in a non-competitive manner. Indeed, the formation of such a ternary complex has been previously reported within live mammalian cells (Ong *et al*., 2001). However, our data suggest otherwise and provide a clearer picture, which may have easily been blurred by the complexity of cellular milieu in the previous study (Ong *et al*., 2001) of the underlying mechanism of the assembly of these macromolecular complexes.

Our study shows that although Grb2 contains two distinct non-overlapping sites for the recruitment of Sos1 and Gab1, the binding of one restricts access to the other so as to favor the formation of two distinct pools of Grb2–Sos1 and Grb2–Gab1 binary complexes in lieu of a composite Sos1–Grb2–Gab1 ternary complex. In this mutually exclusive model, the binding of Sos1 to the nSH3 domain within Grb2 sterically hinders the binding of Gab1 to the cSH3 domain and vice versa. Additionally, our data also suggest that the binding of one partner to Grb2 induces allosteric conformational changes that are likely transmitted to the binding site of the other, causing it to undergo structural disconfiguration and thereby keeping the competing ligand at bay. Our structural models and MD simulations argue that the structurally flexible nature of PR domains of Sos1 and Gab1 is likely to be an important feature of their ability to sterically hinder each other when in association with Grb2 and in causing the latter to undergo conformational changes. Importantly, the binding of both Sos1 and Gab1 to Grb2 is achieved via bivalent interactions mediated by a pair of SH3 recognition motifs within each of these binding partners and by virtue of the fact that Grb2 associates into a homodimer so as to provide a complementary pair of SH3 binding sites for each binding partner. In the case of Sos1, the bivalent interaction is mediated by the binding of two out of four possible PXψPXR motifs (S1/S2/S3/S4) to a pair of nSH3 domains within Grb2 homodimer, while Gab1 binds via both its RXXK motifs (G1/G2) to a pair of cSH3 domains. It is noteworthy that the homodimerization of Grb2 was also recently implicated in the inhibition of basal FGF receptor signaling via steric hindrance (Lin *et al*., 2012).

Given that our analysis was conducted on isolated PR domains of Sos1 and Gab1 in lieu of intact proteins, we cannot rule out that additional factors may also play a role in modulating the binding of these proteins to Grb2 within the milieu of the living cell. In particular, it is now well documented that noise in cellular signaling networks due to the intrinsic promiscuity of protein–protein interactions as well as non-specific weak protein–protein interactions plays a key role in fine-tuning the multimerization

and clustering of signaling components (Ladbury and Arold, 2012). More specifically, it is conceivable that the PR domain within Sos1 does not exist in isolation but rather associates in an intramolecular manner with the neighboring Cdc25/REM catalytic domains required for the activation of Ras in response to RTK stimulation (Boriack-Sjodin *et al*., 1998; Margarit *et al*., 2003). It has indeed been previously shown that the PR domain exerts negative allosteric control on the ability of Sos1 to activate Ras (Corbalan-Garcia *et al*., 1998). Accordingly, intramolecular association of the PR domain of Sos1 may also dictate the extent to which Grb2 binds Sos1 versus Gab1. Additionally, downstream cellular partners of Grb2 may also modulate its access to Sos1 and Gab1 in a competitive and allosteric manner. Thus, the recruitment of Grb2 to the inner membrane surface by virtue of its SH2 domain's ability to bind to pY motifs located within the cytoplasmic tails of a diverse array of RTKs may dictate the competition between Sos1 and Gab1 for Grb2 (Lowenstein *et al*., 1992; Rozakis-Adcock *et al*., 1992; Rozakis-Adcock *et al*., 1993). In T cells, the SH2 domain of Grb2 recognizes pY motifs located on the cytoplasmic tail of the LAT receptor, and such Grb2–LAT interaction could also fine-tune the access of downstream cellular partners of Grb2 (Samelson, 2002). Notably, in addition to Sos1 guanine nucleotide exchange factor and the Gab1 docking protein (Chardin *et al*., 1993; Li *et al*., 1993; Schaeper *et al*., 2000; Lewitzky *et al*., 2001), other well-characterized downstream partners of Grb2 include the dynamin endocytic GTPase (Seedorf *et al*., 1994; Vidal *et al*., 1998), the Cbl ubiquitin ligase (Odai *et al*., 1995; Park *et al*., 1998; Lewitzky *et al*., 2001) and the p27kip1 cell cycle inhibitor (Moeller *et al*., 2003).

We also note that the G1 and G2 motifs flank the binding site for MET and RON receptor tyrosine kinases within the PR domain of Gab1 (Schaeper *et al*., 2000; Schaeper *et al*., 2007; Chaudhuri *et al*., 2011). Given that Gab1 can also be recruited to the inner membrane surface through its direct interaction with the cytoplasmic tails of MET and RON receptors, we believe that Gab1–MET/RON and Gab1–Grb2 interactions are likely to be mutually exclusive via steric hindrance and vice versa. Accordingly, the cellular ratio of Grb2 would likely determine whether the coupling of Gab1 to MET/RON occurs directly or via the Grb2–Gab1 interaction, with important consequences on downstream signaling pathways involved in a diverse array of cellular activities (Schaeper *et al*., 2007; Wagh *et al*., 2008). Interestingly, Sos1 can also be recruited to the inner membrane surface via the binding of its pleckstrin homology (PH) domain to phosphatidic acid (Zhao *et al*., 2007). Thus, membrane recruitment of Gab1 and Sos1 in a Grb2-independent manner represents an alternative facet of cellular signaling and epitomizes the extensive competition between various cellular partners.

In short, our study sheds new light on the role of steric hindrance and allosteric modulation on the formation of multiprotein signaling complexes. Our work therefore lays the groundwork for furthering our understanding of signaling complexes in detailed mechanistic terms. Importantly, our future work will focus on how other cellular partners modulate the formation of Grb2–Sos1 and Grb2–Gab1 complexes.

Acknowledgements

This work was supported by funds from the National Institutes of Health (Grant# R01-GM083897) and the USylvester Braman Family Breast Cancer Institute to AF. CBM is a recipient of a postdoctoral fellowship from the National Institutes of Health (Award# T32-CA119929).

REFERENCES

Adams JA, McGlone ML, Gibson R, Taylor SS. 1995. Phosphorylation modulates catalytic function and regulation in the cAMP-dependent protein kinase. *Biochemistry* **34**: 2447–2454.

Araki T, Nawa H, Neel BG. 2003. Tyrosyl phosphorylation of Shp2 is required for normal ERK activation in response to some, but not all, growth factors. *J. Biol. Chem.* **278**: 41677–41684.

Berendsen HJC, Grigera JR, Straatsma TP. 1987. The Missing Term in Effective Pair Potentials. *J. Phys. Chem.* **91**: 6269–6271.

Boriack-Sjodin PA, Margarit SM, Bar-Sagi D, Kuriyan J. 1998. The structural basis of the activation of Ras by Sos. *Nature* **394**: 337–343.

Carson M. 1991. Ribbons 2.0. *J. Appl. Crystallogr.* **24**: 958–961.

Chardin P, Camonis JH, Gale NW, van Aelst L, Schlessinger J, Wigler MH, Bar-Sagi D. 1993. Human Sos1: a guanine nucleotide exchange factor for Ras that binds to GRB2. *Science* **260**: 1338–1343.

Chardin P, Cussac D, Maignan S, Ducruix A. 1995. The Grb2 adaptor. *FEBS Lett.* **369**: 47–51.

Chaudhuri A, Xie MH, Yang B, Mahapatra K, Liu J, Marsters S, Bodepudi S, Ashkenazi A. 2011. Distinct involvement of the Gab1 and Grb2 adaptor proteins in signal transduction by the related receptor tyrosine kinases RON and MET. *J. Biol. Chem.* **286**: 32762–32774.

Corbalan-Garcia S, Margarit SM, Galron D, Yang SS, Bar-Sagi D. 1998. Regulation of Sos activity by intramolecular interactions. *Mol. Cell. Biol.* **18**: 880–886.

Cunnick JM, Meng S, Ren Y, Desponts C, Wang HG, Djeu JY, Wu J. 2002. Regulation of the mitogen-activated protein kinase signaling pathway by SHP2. *J. Biol. Chem.* **277**: 9498–9504.

Darden TA, York D, Pedersen L. 1993. Particle mesh Ewald: An N.log(N) method for Ewald sums in large systems. *J. Chem. Phys.* **98**: 10089–10092.

Edgcomb SP, Murphy KP. 2000. Structural energetics of protein folding and binding. *Curr. Opin. Biotechnol.* **11**: 62–66.

Egan SE, Giddings BW, Brooks MW, Buday L, Sizeland AM, Weinberg RA. 1993. Association of Sos Ras exchange protein with Grb2 is implicated in tyrosine kinase signal transduction and transformation. *Nature* **363**: 45–51.

Eulenfeld R, Schaper F. 2009. A new mechanism for the regulation of Gab1 recruitment to the plasma membrane. *J. Cell Sci.* **122**: 55–64.

Freire E. 1993. Structural thermodynamics: prediction of protein stability and protein binding affinities. *Arch. Biochem. Biophys.* **303**: 181–184.

Gale NW, Kaplan S, Lowenstein EJ, Schlessinger J, Bar-Sagi D. 1993. Grb2 mediates the EGF-dependent activation of guanine nucleotide exchange on Ras. *Nature* **363**: 88–92.

Gasteiger E, Hoogland C, Gattiker A, Duvaud S, Wilkins MR, Appel RD, Bairoch A. 2005. Protein Identification and Analysis Tools on the ExPASy Server. In The Proteomics Protocols Handbook, Walker JM (ed.). Humana Press: Totowa, New Jersey, USA; 571–607.

Gotoh N. 2008. Regulation of growth factor signaling by FRS2 family docking/scaffold adaptor proteins. *Cancer Sci.* **99**: 1319–1325.

Goudreau N, Cornille F, Duchesne M, Parker F, Tocque B, Garbay C, Roques BP. 1994. NMR structure of the N-terminal SH3 domain of GRB2 and its complex with a proline-rich peptide from Sos. *Nat. Struct. Biol.* **1**: 898–907.

Gu H, Neel BG. 2003. The "Gab" in signal transduction. *Trends Cell Biol.* **13**: 122–130.

Harkiolaki M, Tsirka T, Lewitzky M, Simister PC, Joshi D, Bird LE, Jones EY, O'Reilly N, Feller SM. 2009. Distinct binding modes of two epitopes in Gab2 that interact with the SH3C domain of Grb2. *Structure* **17**: 809–822.

Hess B. 2008. GROMACS 4: Algorithms for Highly Efficient, Load-Balanced, and Scalable Molecular Simulation. *J. Chem. Theory. Comput.* **4**: 435–447.

Hess B, Bekker H, Berendsen HJC, Fraaije JGEM. 1997. LINCS: A linear constraint solver for molecular simulations. *J. Comput. Chem.* **18**: 1463–1472.

Jorgensen WL, Tirado-Rives J. 1988. The OPLS Force Field for Proteins: Energy Minimizations for Crystals of Cyclic Peptides and Crambin. *J. Am. Chem. Soc.* **110**: 1657–1666.

Kaminski GA, Friesner RA, Tirado-Rives J, Jorgensen WL. 2001. Evaluation and Reparametrization of the OPLS-AA Force Field for Proteins via

Comparison with Accurate Quantum Chemical Calculations on Peptides. *J. Phys. Chem. B* **105**: 6474–6487.
Kim D, Chung J. 2002. Akt: versatile mediator of cell survival and beyond. *J. Biochem. Mol. Biol.* **35**: 106–115.
Ladbury JE, Arold ST. 2012. Noise in cellular signaling pathways: causes and effects. *Trends Biochem. Sci.* **37**: 173–178.
Lewitzky M, Kardinal C, Gehring NH, Schmidt EK, Konkol B, Eulitz M, Birchmeier W, Schaeper U, Feller SM. 2001. The C-terminal SH3 domain of the adapter protein Grb2 binds with high affinity to sequences in Gab1 and SLP-76 which lack the SH3-typical P-x-x-P core motif. *Oncogene* **20**: 1052–1062.
Li N, Batzer A, Daly R, Yajnik V, Skolnik E, Chardin P, Bar-Sagi D, Margolis B, Schlessinger J. 1993. Guanine-nucleotide-releasing factor hSos1 binds to Grb2 and links receptor tyrosine kinases to Ras signalling. *Nature* **363**: 85–88.
Lin CC, Melo FA, Ghosh R, Suen KM, Stagg LJ, Kirkpatrick J, Arold ST, Ahmed Z, Ladbury JE. 2012. Inhibition of Basal FGF Receptor Signaling by Dimeric Grb2. *Cell* **149**: 1514–1524.
Lock LS, Royal I, Naujokas MA, Park M. 2000. Identification of an atypical Grb2 carboxyl-terminal SH3 domain binding site in Gab docking proteins reveals Grb2-dependent and -independent recruitment of Gab1 to receptor tyrosine kinases. *J. Biol. Chem.* **275**: 31536–31545.
Lowenstein EJ, Daly RJ, Batzer AG, Li W, Margolis B, Lammers R, Ullrich A, Skolnik EY, Bar-Sagi D, Schlessinger J. 1992. The SH2 and SH3 domain-containing protein GRB2 links receptor tyrosine kinases to ras signaling. *Cell* **70**: 431–442.
Maignan S, Guilloteau JP, Fromage N, Arnoux B, Becquart J, Ducruix A. 1995. Crystal structure of the mammalian Grb2 adaptor. *Science* **268**: 291–293.
Margarit SM, Sondermann H, Hall BE, Nagar B, Hoelz A, Pirruccello M, Bar-Sagi D, Kuriyan J. 2003. Structural evidence for feedback activation by Ras.GTP of the Ras-specific nucleotide exchange factor SOS. *Cell* **112**: 685–695.
Marti-Renom MA, Stuart AC, Fiser A, Sanchez R, Melo F, Sali A. 2000. Comparative Protein Structure Modeling of Genes and Genomes. *Annu. Rev. Biophys. Biomol. Struct.* **29**: 291–325.
McDonald CB, Seldeen KL, Deegan BJ, Farooq A. 2008a. Structural basis of the differential binding of the SH3 domains of Grb2 adaptor to the guanine nucleotide exchange factor Sos1. *Arch. Biochem. Biophys.* **479**: 52–62.
McDonald CB, Seldeen KL, Deegan BJ, Farooq A. 2008b. Structural Basis of the Differential Binding of the SH3 Domains of Grb2 Adaptor to the Guanine Nucleotide Exchange Factor Sos1. *Arch. Biochem. Biophys.* **479**: 52–62.
McDonald CB, Seldeen KL, Deegan BJ, Lewis MS, Farooq A. 2008c. Grb2 adaptor undergoes conformational change upon dimerization. *Arch. Biochem. Biophys.* **475**: 25–35.
McDonald CB, Seldeen KL, Deegan BJ, Farooq A. 2009a. SH3 Domains of Grb2 Adaptor Bind to PXpsiPXR Motifs Within the Sos1 Nucleotide Exchange Factor in a Discriminate Manner. *Biochemistry* **48**: 4074–4085.
McDonald CB, Seldeen KL, Deegan BJ, Farooq A. 2009b. SH3 domains of Grb2 adaptor bind to PXpsiPXR motifs within the Sos1 nucleotide exchange factor in a discriminate manner. *Biochemistry* **48**: 4074–4085.
McDonald CB, Seldeen KL, Deegan BJ, Bhat V, Farooq A. 2010. Assembly of the Sos1-Grb2-Gab1 ternary signaling complex is under allosteric control. *Arch. Biochem. Biophys.* **494**: 216–225.
McDonald CB, Seldeen KL, Deegan BJ, Bhat V, Farooq A. 2011. Binding of the cSH3 domain of Grb2 adaptor to two distinct RXXK motifs within Gab1 docker employs differential mechanisms. *J. Mol. Recognit.* **24**: 585–596.
McDonald CB, Balke JE, Bhat V, Mikles DC, Deegan BJ, Seldeen KL, Farooq A. 2012a. Multivalent binding and facilitated diffusion account for the formation of the Grb2-Sos1 signaling complex in a cooperative manner. *Biochemistry* **51**: 2122–2135.
McDonald CB, Bhat V, Mikles DC, Deegan BJ, Seldeen KL, Farooq A. 2012b. Bivalent binding drives the formation of the Grb2-Gab1 signaling complex in a noncooperative manner. *FEBS J.* **279**: 2156–2173.
Moeller SJ, Head ED, Sheaff RJ. 2003. p27Kip1 inhibition of GRB2-SOS formation can regulate Ras activation. *Mol. Cell. Biol.* **23**: 3735–3752.
Murphy KP. 1999. Predicting binding energetics from structure: looking beyond DeltaG degrees. *Med. Res. Rev.* **19**: 333–339.
Murphy KP, Freire E. 1992. Thermodynamics of structural stability and cooperative folding behavior in proteins. *Adv. Protein Chem.* **43**: 313–361.
Nimnual A, Bar-Sagi D. 2002. The two hats of SOS. *Sci. STKE* **2002**: PE36.
Odai H, Sasaki K, Iwamatsu A, Hanazono Y, Tanaka T, Mitani K, Yazaki Y, Hirai H. 1995. The proto-oncogene product c-Cbl becomes tyrosine phosphorylated by stimulation with GM-CSF or Epo and constitutively binds to the SH3 domain of Grb2/Ash in human hematopoietic cells. *J. Biol. Chem.* **270**: 10800–10805.
Ong SH, Hadari YR, Gotoh N, Guy GR, Schlessinger J, Lax I. 2001. Stimulation of phosphatidylinositol 3-kinase by fibroblast growth factor receptors is mediated by coordinated recruitment of multiple docking proteins. *Proc. Natl. Acad. Sci. U. S. A.* **98**: 6074–6079.
Park RK, Kyono WT, Liu Y, Durden DL. 1998. CBL-GRB2 interaction in myeloid immunoreceptor tyrosine activation motif signaling. *J. Immunol.* **160**: 5018–5027.
Reuther GW, Der CJ. 2000. The Ras branch of small GTPases: Ras family members don't fall far from the tree. *Curr. Opin. Cell Biol.* **12**: 157–165.
Robinson MJ, Cobb MH. 1997. Mitogen-activated protein kinase pathways. *Curr. Opin. Cell Biol.* **9**: 180–186.
Rozakis-Adcock M, McGlade J, Mbamalu G, Pelicci G, Daly R, Li W, Batzer A, Thomas S, Brugge J, Pelicci PG, Schlessinger J, Pawson T. 1992. Association of the Shc and Grb2/Sem5 SH2-containing proteins is implicated in activation of the Ras pathway by tyrosine kinases. *Nature* **360**: 689–692.
Rozakis-Adcock M, Fernley R, Wade J, Pawson T, Bowtell D. 1993. The SH2 and SH3 domains of mammalian Grb2 couple the EGF receptor to the Ras activator mSos1. *Nature* **363**: 83–85.
Samelson LE. 2002. Signal transduction mediated by the T cell antigen receptor: the role of adapter proteins. *Annu. Rev. Immunol.* **20**: 371–394.
Schaeper U, Gehring NH, Fuchs KP, Sachs M, Kempkes B, Birchmeier W. 2000. Coupling of Gab1 to c-Met, Grb2, and Shp2 mediates biological responses. *J. Cell Biol.* **149**: 1419–1432.
Schaeper U, Vogel R, Chmielowiec J, Huelsken J, Rosario M, Birchmeier W. 2007. Distinct requirements for Gab1 in Met and EGF receptor signaling in vivo. *Proc. Natl. Acad. Sci. U. S. A.* **104**: 15376–15381.
Seedorf K, Kostka G, Lammers R, Bashkin P, Daly R, Burgess WH, van der Bliek AM, Schlessinger J, Ullrich A. 1994. Dynamin binds to SH3 domains of phospholipase C gamma and GRB-2. *J. Biol. Chem.* **269**: 16009–16014.
Spolar RS, M.T. Record J. 1994. Coupling of local folding to site-specific binding of proteins to DNA. *Science* **263**: 777–784.
Terasawa H, Kohda D, Hatanaka H, Tsuchiya S, Ogura K, Nagata K, Ishii S, Mandiyan V, Ullrich A, Schlessinger J, Inagaki F. 1994. Structure of the N-terminal SH3 domain of GRB2 complexed with a peptide from the guanine nucleotide releasing factor Sos. *Nat. Struct. Biol.* **1**: 891–897.
Toukan K, Rahman A. 1985. Molecular-dynamics study of atomic motions in water. *Physical. Review. B.* **31**: 2643–2648.
Van Der Spoel D, Lindahl E, Hess B, Groenhof G, Mark AE, Berendsen HJ. 2005. GROMACS: fast, flexible, and free. *J. Comput. Chem.* **26**: 1701–1718.
Vidal M, Montiel JL, Cussac D, Cornille F, Duchesne M, Parker F, Tocque B, Roques BP, Garbay C. 1998. Differential interactions of the growth factor receptor-bound protein 2 N-SH3 domain with son of sevenless and dynamin. Potential role in the Ras-dependent signaling pathway. *J. Biol. Chem.* **273**: 5343–5348.
Wagh PK, Peace BE, Waltz SE. 2008. Met-related receptor tyrosine kinase Ron in tumor growth and metastasis. *Adv. Cancer Res.* **100**: 1–33.
Wiseman T, Williston S, Brandts JF, Lin LN. 1989. Rapid measurement of binding constants and heats of binding using a new titration calorimeter. *Anal. Biochem.* **179**: 131–137.
Wittekind M, Mapelli C, Farmer BT, 2nd, Suen KL, Goldfarb V, Tsao J, Lavoie T, Barbacid M, Meyers CA, Mueller L. 1994. Orientation of peptide fragments from Sos proteins bound to the N-terminal SH3 domain of Grb2 determined by NMR spectroscopy. *Biochemistry* **33**: 13531–13539.
Wittekind M, Mapelli C, Lee V, Goldfarb V, Friedrichs MS, Meyers CA, Mueller L. 1997. Solution structure of the Grb2 N-terminal SH3 domain complexed with a ten-residue peptide derived from SOS: direct refinement against NOEs, J-couplings and 1H and 13C chemical shifts. *J. Mol. Biol.* **267**: 933–952.
Xie D, Freire E. 1994. Molecular basis of cooperativity in protein folding. V. Thermodynamic and structural conditions for the stabilization of compact denatured states. *Proteins* **19**: 291–301.
Yart A, Laffargue M, Mayeux P, Chretien S, Peres C, Tonks N, Roche S, Payrastre B, Chap H, Raynal P. 2001. A critical role for phosphoinositide 3-kinase upstream of Gab1 and SHP2 in the activation of ras and mitogen-activated protein kinases by epidermal growth factor. *J. Biol. Chem.* **276**: 8856–8864.
Zhao C, Du G, Skowronek K, Frohman MA, Bar-Sagi D. 2007. Phospholipase D2-generated phosphatidic acid couples EGFR stimulation to Ras activation by Sos. *Nat. Cell Biol.* **9**: 706–712.

